Influence of surface pre-treatment in the formation of nanoporous alumina

D. C. Leitão [a,*], C. T. Sousa [a,b], J. Ventura [a], F. Carpinteiro [a], J. G. Correia [b], M. M. Amado [a], J. B. Sousa [a], J. P. Araújo [a]

[a] *IN - Unidade IFIMUP, Rua do Campo Alegre, 678, 4169-007 Porto,Portugal*

[b] *ITN, EN 10, Lisbon, Portugal*

Abstract

In nanoporous alumina, surface pre-treatment, prior to the anodization process, plays a crucial role in the pore structure formation and organization. In this work we employ different pre-treatments to determine the best suited for the subsequent anodization process. We observed significative differences in the current density transients (monitored during anodization), depending on the pre-treatment used. For diamond paste polished surface, scanning electron microscope (SEM) images of the first anodization revealed a degraded porous structure, with no organization. Samples with NaOH soft chemical etching, ion milling etching and electropolishing pre-treatments revealed the best quality first anodization surfaces, so that a second anodization process was applied. Current density transients, together with SEM images, showed that there was still growth competition for the ion-milling and electropolishing cases and longer first anodization times are thus required to obtain the equilibrium structure. For NaOH soft chemical etching, we conclude that the dimples carved in the aluminum foil from the first anodization step act as nucleation sites for the second anodization porous structure.

Key words: nanoporous alumina, anodization, pre-treatment
PACS:

1 Introduction

Nanoporous materials have gained much importance in the last 20 years due to their potencial industrial and technological applications for nanometric device

* Corresponding author.
Email address: dleitao@fc.up.pt (D. C. Leitão).

fabrication. In fact, the existing nano-lithographic techniques like e-beam, X-ray or focused ion beam are expensive and have a low throughput, and thus one needs new assembling methods for the large scale and inexpensive production of nanodevices. Self-assembled nanoporous alumina can be readily obtained by common electrochemical processes, well known to the chemical industries, and can be used to achieve the required nanodimensions. The unique properties, low-cost processing and compatibility with existing semiconductor microfabrication technologies make anodic aluminum oxide (AAO) a promising candidate for the template-based growth of nanostructures. Applications such as nanodots (antidots) [1], nanochannels [2], nanowires [3] or photonic crystals [4] evidence the versatility and potential of AAO templates. The arrangement and size of the pores depend on the applied anodization potential, anodization temperature, type and concentration of the electrolyte. Highly-ordered hexagonal lattices have been successfully prepared by a two-step anodization process [5] and structures with pore diameters in the 24-158 nm range and inter-pore distances between 66-500 nm were demonstrated [6]. Furthermore, different ordered pore structures, such as square and triangular lattices, have been obtained by means of pre-patterning techniques [6].

Previous studies showed the influence of surface pre-treatment on the AAO self-ordering using organic acids (such as oxalic, malonic or tartaric) as electrolytes [7,8]. It was shown that the formation of both barrier oxide layer and pores is faster in a surface with a high roughness. However, this also gives rise to a rough etching front, preventing self-organization [7]. On the other hand it was found that electropolishing alone is not a suitable pre-treatment when low dissociation constant acids are used [8]. Electropolishing must then be followed by an alkaline treatment [8] or by a hard anodization in oxalic acid [9].

In this work we concentrate on sulphuric acid anodizations and study how different pre-treatments of the aluminum foils (etanol degreasing, chemical etching in 1M NaOH, diamond paste polishing, electropolishing and ion-milling etching, all compared to an as-rolled samples) influence pores growth and organization. Anodizations were carried out in 1.2 M H_2SO_4 at a constant potential of 15 V for 1 hour, at room temperature. The current transients were monitored during anodization, allowing us to probe pore formation. After the first anodization we observed the top of the anodized foil (alumina surface). We then removed this alumina layer to observe the pattern formed at the underlying aluminum surface. Scanning Electron Microscopy (SEM) images were then obtained after the second anodization (under the same conditions as the first). Our data allowed us to probe the influence of different pre-treatments in the porous structure. After the first anodization, we found that NaOH soft chemical etching, ion-milling and electropolishing gave adequate surfaces for a second anodization. However, from these, both ion-milled and electropolished samples still showed pore growth competition during the second anodization.

On the other hand, pre-treatment using NaOH chemical etching results in a direct growth of pores guided by first anodization nucleation sites.

2 Experimental details

The nanoporous alumina samples were fabricated by anodization of high purity aluminum foils (99.997%), with a home-made anodization cell [10]. The anodized area was about 30 mm^2. Prior to the anodization process the as-rolled samples were degreased in C_2H_5OH for 5 minutes, in an ultra-sound bath. Different pre-treatments were then employed: soft chemical etching for 5 minutes in 1 M NaOH, enabling the removal of the native oxide layer (sample S_{NaOH}); diamond paste polishing (S_{diam}); soft chemical etching (1 M NaOH) followed by ion-milling, in a CSC Ion Beam Sputter, with 5.0 sccm Ar flow at 1000 V beam voltage, for 1 hour (S_{mill}); and electropolishing in a $HClO_4$:C_2H_5OH solution (ratio 1:4) at 12°C, with a 28 V potential applied for 1 minute ($S_{electro}$). For comparison, samples without any pre-treatment were also anodized ($S_{control}$). First anodizations were carried out in 1.2 M H_2SO_4 with a constant potential of 15 V, for 1 hour at room temperature. Afterwards, the alumina layer was removed with a 0.4 M H_3PO_4:0.2M $HCrO_4$ solution, at 60°C during 15 minutes. SEM analysis confirmed the presence of dimples in the bottom aluminum foils, arising from the nanoporous alumina layer formed during anodization. To obtain better organized structures, a two-step anodization method [5] was employed. Therefore, a second anodization of the aluminum (over the carved hole structure) was then carried out using the same conditions as the first one. Current density transients were monitored during the anodization processes using a home-made LabView program that controls a Keithley *2004 Sourcemeter*, enabling current measurements while applying the constant anodization potential.

3 Experimental results

Figure 1(a) shows the current density transients [*j(t)*], monitored during the first anodization step, for all the studied samples ($S_{control}$, S_{NaOH}, S_{diam}, $S_{electro}$ and S_{mill}). Typical behavior, indicative of porous structure formation [11], was observed and confirmed by low-vacuum SEM analysis (see below). The initial decrease in *j(t)*, corresponds to the formation of a continuous alumina layer (high resistance). Then, field-enhanced oxide dissolution starts to occur in regions where irregularities on the surface are present; *j(t)* reaches a minimum value, when oxide-growth is balanced by oxide-dissolution. Afterwards *j(t)* increases towards a local maximum, corresponding to the initial

stage of pore nucleation and growth. Finally, due to growth competition among the pores, *j(t)* again slightly decreases, ultimately reaching a steady-state value indicative of an equilibrium between aluminum oxide-dissolution (at the electrolyte/oxide interface) and aluminum oxide-growth (at the metal/oxide interface), giving a constant pore growth rate, and constant *j(t)*.

Significative differences can be observed in the *j(t)* maximum values for the first anodization, depending on the employed pre-treatment. Whereas in electropolishing and soft chemical etching samples, a $j(t)$-j^{i}_{min} maximum around 11.9 mA/cm^2 and 8.5 mA/cm^2 is observed, respectively, lower values of 6.5 mA/cm^2, 6.4 mA/cm^2 and 4.7 mA/cm^2 were found for diamond paste polishing, control sample and ion-milling etching, respectively [Fig. 1(a)]. In the case of samples $S_{control}$, S_{diam}, S_{NaOH}, expected to have rougher surfaces, large size pores nucleate at irregularities in the aluminum surface [12]. This correlates well with the observed *j(t)* behaviors, where the maxima are not too pronounced.

In samples with smother surfaces (S_{mill} and $S_{electro}$), there is initially a large number of small pores nucleating due to the virtual absence of irregularities on the surface [12]. As a result, *j(t)* exhibits a drastic rise, until it reaches the maximum value. On the other hand, such large number of pores will give rise to a larger competition among them, thus leading to the observed sharp decrease after *j(t)* maximum. This expected behavior is more noticeable in $S_{electro}$ than in S_{mill}. This maybe due to the existence of defects introduced during the ion-milling process which will act as preferential pore nucleation sites. In order to check this, anodization of ion milled foils after annealing would be necessary.

SEM images after the first anodization revealed not only the expected porous structure inferred from the *j(t)* curves, but also the quality of the surface. Figure 2 shows SEM images of the porous alumina surface after first anodization for samples with different pre-treatments. Figures 2(a) and 2(b) correspond to samples $S_{control}$ and S_{diam}, respectively. Both reveal an irregular surface and a very degraded porous structure. On the other hand, samples S_{NaOH}, S_{mill} and $S_{electro}$ [Fig.2(c)-(e), respectively], exhibit a rather smooth surface, with well defined pores, without an organized structure likely because the anodizations were performed at room temperature.

After removal of the first porous alumina layer, the templates, having a patterned hole structure, were again anodized. In this second anodization [Fig.1(b); only performed in $S_{electro}$, S_{mill} and S_{NaOH}], we observe that the current decrease after *j(t)* maximum is less pronounced. In fact, for S_{NaOH}, there is no such decrease after *j(t)* maximum, while for the other samples a small change is visible. This indicates that pore-growth competition is still active during the second anodization for S_{mill} and $S_{electro}$. As these samples have

smoother surfaces and more pores were nucleated, longer first anodization times would be required for the equilibrium state to be reached.

Figures 3(a)-(c) show SEM alumina surface images of the fabricated samples after a second anodization step. A more organized pore structure can be observed when compared with the first anodization surfaces [Figs.2(c)-(d)]. Pore diameters of ∼15 nm and a center-to-center inter-pore distance of ∼65 nm are observed. However, the ordered regions are still small (less then 100x100 nm^2) and do not hold a well defined hexagonal lattice. Lower temperatures and longer first anodization times are required to obtain such results, which are not the issues of this work.

From the SEM images we can conclude that, with the anodization conditions employed (1.2 M H_2SO_4; U = 15 V; 1 hour anodization time at room temperature) a pre-treatment with NaOH etching gives better results with a good quality surface and, to a certain extent, organized pore structures. This can also be seen in the second anodization *j(t)* curves [Fig.1(b)], for which no decrease after the maximum value was observed for S_{NaOH}. This result points to a direct growth of pores guided by the first anodization nucleation sites. On the contrary, for samples S_{mill} and $S_{electro}$ the existence of a decrease in *j(t)* indicates that there was still some pore growth competition, i.e. the porous structure had not reached an equilibrium during first anodization, thus resulting in a not organized porous structure [Fig.3(c) and 3(d)]. The small first anodization time and relatively high temperature, may be the reasons why the pores did not reach an equilibrium and thus a well organized structure. This relates to the fact that in smoother surfaces, a larger number of pores nucleate, so longer anodization times are necessary to obtain the desired organized structure.

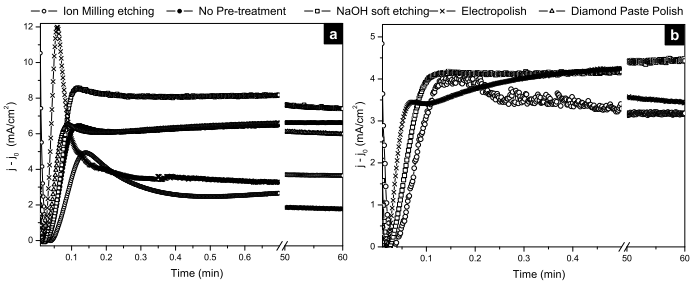

Fig. 1. Current density transients [*j(t)*] monitored during the anodization process. (a) Comparison of the first anodization process for all samples; (b) comparison of the second anodization process for samples $S_{electro}$, S_{mill} and S_{NaOH}. For comparison purposes the minimum value of *j(t)* (j^i_{min}) was subtracted to each curve.

4 Conclusions

Different surface pre-treatments were considered and their influence in the pore structure and organization upon anodization at room temperature was studied. Diamond paste polishing pre-treatment revealed a very degraded pore structure after the first anodization step. Scanning Electron Microscopy images after the second anodization allowed us to conclude that a pre-treatment

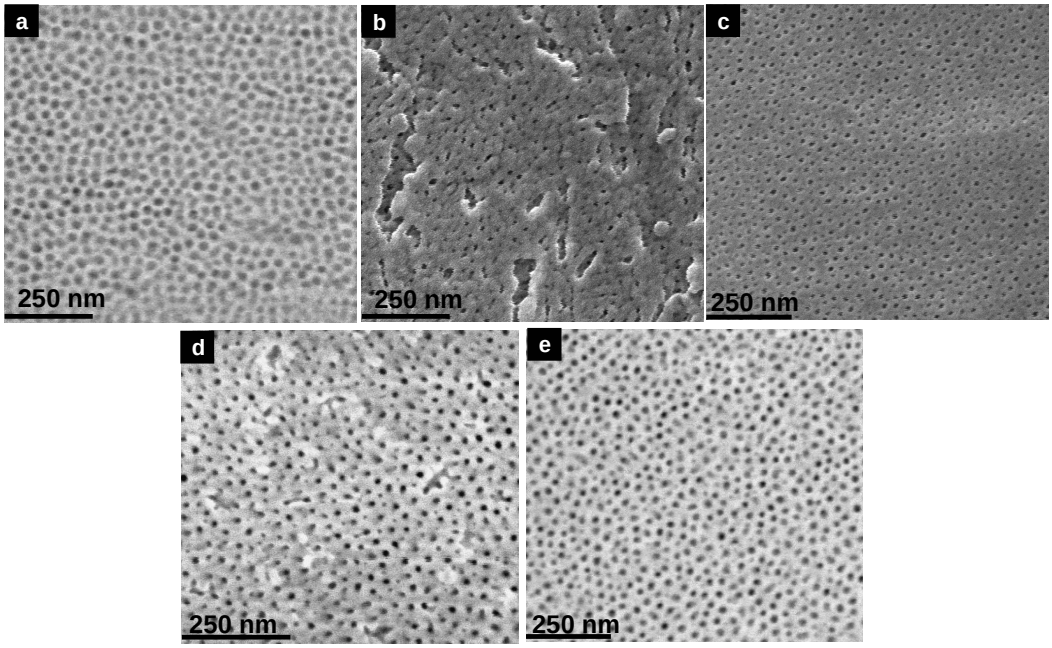

Fig. 2. Low-vacuum SEM images for all samples after first anodization (a) $S_{control}$; (b) S_{diam}; (c) S_{NaOH} ; (d) S_{mill}; (e) $S_{electro}$. Anodization was performed in a 1.2 M H_2SO_4 solution under an applied constant potencial of 15 V, for 1 hour, at room temperature.

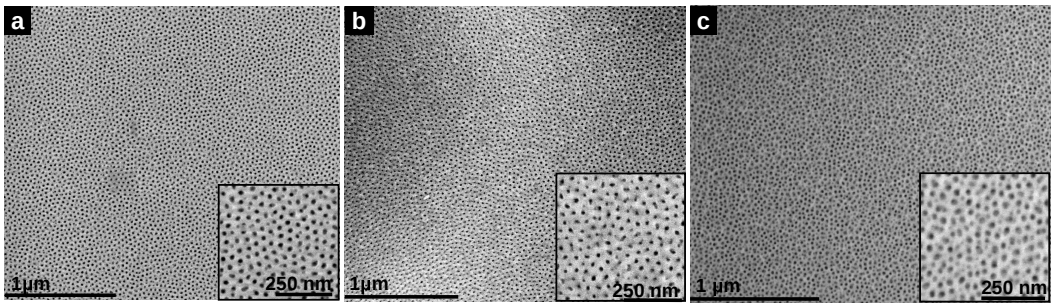

Fig. 3. Second anodization (under the same conditions as the first one) SEM images for samples (a) S_{NaOH}, (b) S_{mill} and (c) $S_{electro}$.

with NaOH etching results in the direct growth of pores guided by the first anodization nucleation sites (for 1 h anodization time). On the contrary, samples S_{mill} and $S_{electro}$ still show pore-growth competition, likely due to the small first anodization time.

Acknowledgements

D.C.Leitao and C.T.Sousa are thankful to FCT for doctoral grant SFRH/BD/25536/2005 and ITN for PDCT/FP/63911/2005. We also thank to the Fundacao Gulbenkian for their financial support within the "Programa Gulbenkian de Estimulo a Investigacao Cientifica".

References

[1] Z. L.Xiao, C. Han, U. Welp, H. Wang, V. Vlasko-Vlasko, W. Kwok, D. Miller, J. Hiller, R. Cook, G. Willing and G. Crabtree, Appl. Phys. Lett. 81 (2002) 2869.

[2] D. Navas, M. Hernández-Vlez, M. Vazquez, W. Lee and K. Nielsch, Appl. Phys. Lett. 90 (2007) 192501.

[3] K. Nielsch, F. Mller, A.P. Li and U. Gsele, Adv. Mat. 12 (2000) 582-586

[4] H. Masuda, H. Asoh, M. Watanabe, K. Nishio, M. Nakao and T. Tamamura, Adv. Mat. 13 (2001) 189-192.

[5] H. Masuda and K. Fukuda, Science 268 (1995) 146.

[6] W. Lee, R. Ji, U. Gösele and K. Nielsch, Nat. Mat. 5 (2006) 741.

[7] O. Jessensky, F. Muller and U. Gosele, J. Electrochem. Soc. 145 (1998) 3735.

[8] S. Ono, M. Saito and H. Asoh, Electrochem. Acta 51 (2005) 827.

[9] W. Lee, K. Nielsh and U. Gosele, Nanotechnology 18 (2007) 475713.

[10] C.T. Sousa, D.C. Leitao,J. Ventura, A.M. Pereira, J.G. Correia, M.M. Amado, J.B. Sousa and J.P. Araújo, 8ENCMP Procedings (2007); http://www2.fc.up.pt/pessoas/jearaujo/

[11] J.W Diggle, T.C. Downie and C.W. Goulding, Chem. Rev. 69 (1969) 365-405 (2005).

[12] G.E. Thompson, Thin Sol. Films 297 (1997) 192-201.